Aerospace Science and Technology 68 (2017) 345–361

Contents lists available at ScienceDirect

Aerospace Science and Technology

www.elsevier.com/locate/aescte

Aircraft engine health prognostics based on logistic regression with penalization regularization and state-space-based degradation framework

Jianbo Yu

School of Mechanical Engineering, Tongji University, Shanghai, 201804 PR China

ARTICLE INFO

Article history:
Received 4 September 2016
Received in revised form 8 April 2017
Accepted 23 May 2017
Available online 26 May 2017

Keywords:
Engine health prognostics
Remaining useful life
Logistic regression
Penalization regularization
State-space-model
Particle filtering

ABSTRACT

Engine health prognostics is critical to ensure reliability and safety of aircraft operations due to the provision of various health decision information. In this studying, a prognostics system is developed based on logistic regression (LR) and state-space-model (SSM) for engine health assessment and prediction. In this system, a health indicator based on logistic probability (LP) inferred from a variable set of sensor signals selected by LR with penalization regularization (LRPR) is used to characterize engine health states. LP is capable of offering a failure probability for the monitored engine, which has intuitive explanation related to its health state. A data-model-fusion method is developed for the engine health prognostics task accomplished by integration of LR and particle filtering (PF). Bayesian state estimations, on the basis of the engine health changes modeled by a baseline LR, are implemented to sequentially update the current health state and then to predict the future health propagation of engines. The prognostics system is applied to a gas turbine on the Commercial Modular Aero-Propulsion System Simulation (C-MAPSS) test-bed developed by NASA. The experimental results indicate the potential applications of the proposed system as an effective tool for engine health prognostics.

1. Introduction

Prognostics and health management (PHM) is an effective maintenance technique to achieve reliable and safety operation of machines and systems. The emphasis of this studying field has been focused on assessment and prediction of machine health, so those breakdowns can be predicted and prevented effectively [1–6]. To fulfill the goal of machine health prognostics, the following three crucial steps are generally implemented in a prognostics system. First, the health degradation of machines can be detected and identified as early as possible. Second, the health propagation of machines should be quantified and tracked continuously over time series flow. Finally, the remaining useful life (RUL) of machines can be effectively predicted to offer important health information to users.

Nevertheless, a gas turbine engine is a very complex large-scale system whose subsystems (or components) are interconnected physically [2]. Kurz and Brun [7] discussed the effect of engine health deterioration on the package as part of a complex system based on some mechanisms that cause health changes. It is a challenging task to implement health prognostics in the system level of engines, which has been addressed by many investigators over the last several decades. The first challenge is to construct an effective monitoring model for online quantifying engine health states. Recently, some methods have been developed for engine health assessment and prediction [8–15]. Nieto et al. [8] developed a hybrid PSOSVM-based method for forecasting of aircraft engine health. Li and Nilkitsaranont [9] employed implanted compressor efficiency degradation to describe the health states of gas turbines. Nonlinear principal component analysis (PCA)-based statistic indication was used to detect faults of diesel engines [10]. Artificial neural networks (ANNs) were applied for assessing the deteriorated component characteristics in micro gas engine [11]. Gupta et al. [12] employed symbolic dynamic filtering (SDF) for fault detection and isolation in gas turbine engines. Sun et al. [4] proposed a linear or nonlinear regression model to construct a health indicator for quantifying engine health states. An obvious defect of these models is that they can not provide a health indicator with a determined range, e.g., [0 1] to provide consistent quantification values for different engines (or components), which could limit their wide applications in the real-world cases. In addition, a good health indicator must not only capture the physical

E-mail address: jianboyu.bob@gmail.com.

http://dx.doi.org/10.1016/j.ast.2017.05.030
1270-9638/

Notation

$P(x)$	Logistic prediction probability
$g(x)$	Logit model
β	The vector of regression coefficients
X	The input/training feature mixture
Y	The output
$LR()$	Logistic regression model
δ_s	The threshold of slight degradation
δ_f	The threshold of engine failure
x_k	The system state
y_k	The system output
f_k	A state transition function
h_k	A possibly nonlinear function
ω_k	The system state noise
v_k	The system output noise
$p(x_k \mid y_{1:k})$	The posterior distribution
w_k^i	The importance weight of the particle i
t_k	The engine age
N	The number of particles
$\tilde{x}_{k+h}$	The h-steps-ahead prediction
$F(k)$	The cumulative failure distribution function
k	The time point
$N(\mu_\omega^k, \sigma_\omega^k)$	A Gaussian distribution for the Markov process noise ω_k

transitions that the engine undergoes during different stages of its life, but must also be easy to use in an actual situation. Thus, the failure probability-based health indicator with a determined range (0–1) could improve the effectiveness of the engine health prognostics system.

The other big challenge is engine RUL prediction to implement effective maintenance, which needs knowledge of high-accuracy prediction. The existing machine RUL prediction models can be generally classified into two categories, namely, model-based method and data-driven method. Model-based methods typically involve building models to estimate physical characteristics of machine failure modes. They, however, may not be suitable for many industrial applications in which these physical parameters and fault modes may vary dynamically under different working conditions. Some typical model-based methods have been developed for engine health estimation and RUL prediction [13–17]. If properly used, model-based methods are capable of improving accuracy of engine RUL prediction, significantly. However, those engine failure processes are typically complicated and dynamic, and authentic model-based models are very difficult to construct for engine health prognostics.

In recent years, Bayesian theory-based framework has been used to model the engine health degradation and predict the RUL. Kalman filtering (KF) seems to be the most commonly used method for engine health estimation. Simon [18] performed a comparison of the filtering approaches including linearized KF (LKF), extended KF (EKF) and unscented KF (UKF) for engine health estimation and prediction. The constrained KF (CKF) was also used for turbofan engine health estimation [19]. Simon and Garg [20] further analyzed optimal turner selection for KF-based engine health estimation method. Lu et al. [21] proposed an improved EKF with inequality constraints for gas turbine engine health monitoring. Pourbabaee et al. [22] proposed a multiple-model-based hybrid KF for sensor fault detection, isolation, and identification of gas turbine engines. Recently, particle filtering (PF) has been applied in machine health prognostics since their health degradation is a nonlinear problem while PF is particularly useful in dealing with this issue [4,23,24]. Some combinations of PF and predictors (e.g., Gaussian process regression (GPR), support vector regression (SVR), ANN, kernel smoothing, linear regression) are proposed for machine health prediction [4,25–27]. However, a limitation associated with the classical KF and PF-based predictors is that the model parameters (e.g., the state transition function when solving Bayesian recursive state-estimation problem of state-space-mode (SSM)) cannot be updated online during the prognostic period since no new measurements are available, which could decrease their prediction accuracy and then limit their applications in real-world cases.

On the other hand, data-driven method does not require assumption of physical parameters that is difficult to obtain, thus it is easy to use in real-world applications. But this technique generally needs historic data to make the prognostics system as close to real applications as possible. A few techniques based on data-driven models have been reported in literature for engine RUL prediction [28–33], and they are summarized as statistical model, artificial neural network (ANN), support vector machine (SVM), evolutionary prognostics, fuzzy logic, etc. Linear modeling for engine health degradations is one of the prognostic methods and has been employed for short-term prediction of engine health changes [34]. Linear regression-based prediction methods have an obvious limitation that they could only be acceptable for short-term prediction. The combination of linear and nonlinear regression-based prognostic methods for the prediction of engine health into the future was investigated in [35]. Some machine learning methods (e.g., relevance vector machines (RVM)) and nonlinear regression are combined for machine RUL prediction [36–38]. In general, the performance of these data-driven RUL prediction models depends on the effectiveness of health indicators. Furthermore, the data-model-fusion scheme is very interesting, which can take advantage of the strengths of each other while overcoming their respective disadvantages.

Driving by the desire of improved engine uptime and near-zero breakdown productivity, we develop a novel prognostics system to implement on-line engine health assessment and prediction. This system derives a logistic probability (LP) as an effective health indicator based on failure risk probability with a determined range, i.e., 0–1. Based on the LPs on time series flow, an SSM is applied to the dynamics of the engine health changes. Engine RUL prediction is performed through using the PF model, where a combination of the logic regression (LR) predictor and the process noise is applied to represent the health degradation process. The integration of the LR and the PF in this prognostics system aims to solve some important issues like non-linear mapping, real-time state estimation, adaptive learning. Due to the power of LR in pattern recognition and regression prediction, it plays a key role in the proposed prognostics system: (1) LR with penalization regularization (LRPR)-based prognostic feature selection method is proposed for improving the prognostic performance of the proposed system; (2) An LR-based health indicator is developed to quantify engine health states; (3) An LR is integrated in the PF for engine RUL prediction. With the health indicator and RUL prediction results, users will obtain important information about the engine health state and failure time, and then take correct and timely maintenance measurements to recover the engine health. Thus, the proposed prognostics system provides an effective methodology of enhancing the assessment and prediction of engine health degradation. Therefore, the major contributions and innovations of

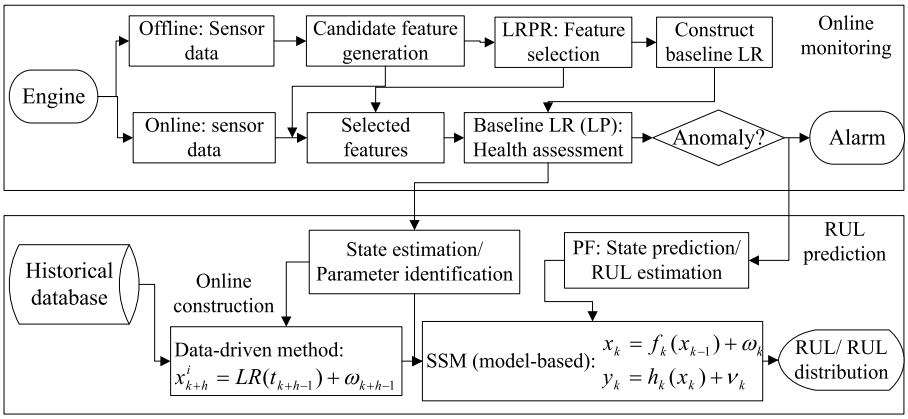

Fig. 1. The schematic diagram of engine health prognostics.

this paper include: (1) LRPR-based prognostic feature selection and LR-based health indicator are proposed to improve the assessment performance of the proposed prognostics system for engine health degradation significantly; (2) The proposed prognostic framework integrating the model-based method (i.e., PF) and the data-driven method (i.e., LR) obtains strengths of each method while overcoming their respective disadvantages; (3) A whole methodology for engine health assessment and prediction is finally developed to provide the important prognostic information (i.e., health indicator, health prediction and RUL prediction) to users. The experimental results validate feasibility of the proposed prognostics system on the gas turbine engine of Commercial Modular Aero-Propulsion System Simulation (C-MAPSS) test-bed developed by NASA.

The rest of the paper is organized as follows. Section 2 proposes an engine health prognostics system. Section 3 proposes an LR-based engine health assessment and prediction method. An integration model of LR and PF for engine RUL prediction is developed in Section 4. An experiment is performed on engine life test-bed to illustrate the effectiveness of the proposed prognostics system in Section 5. Conclusions are given in Section 6.

2. Engine health prognostics system

The engine health prognostics procedure fuses and utilizes the historic information present in sensor variables with the objective of assessing and determining the running conditions (states) of the engine and further estimating its health propagation in future. From a nonlinear Bayesian state prediction standpoint, this may be accomplished by the use of a nonlinear dynamic state model. As a summary, the schematic diagram of the proposed engine health prognostics system is presented in Fig. 1. The proposed system consists of two key parts, i.e., online engine health monitoring and RUL prediction (see upper and the lower boxes in Fig. 1, respectively). In the offline modeling phrase, sensor data are collected for the system modeling. Then, this system uses an LRPR-based prognostic feature selection method for improving prognostic performance of the proposed system. A health indicator (i.e., LP) generated by a baseline LR is developed to quantify engine health states. In the online prognostic phrase, the collected sensor data online are input the baseline LR to generate LP to determine the health state of the engine. If the LP indicator triggers a health degradation alarm, a Bayesian estimation of SSM is developed for modeling health propagation of engines on time series flow. The LR predictor, as the health degradation model, is integrated with a PF model to form a data-model-fusion framework for engine RUL prediction.

3. Logistic regression-based engine health assessment and prediction

3.1. Logistic regression with penalization regularization

LR has been used widely in time-series prediction, pattern recognition, etc. [39]. In this studying, LR is further extended to applications of feature selection, health assessment and RUL prediction in the proposed engine health prognostics system. LR is an effective method to find the best fitting model to describe the nonlinear relationship between the categorical characteristic of dependent variable and a set of independent variables [39]. Its logistic prediction probability for an event occurrence is constrained between 0 and 1:

$$P(x) = \frac{1}{1 + e^{-g(x)}} \tag{1}$$

where $g(x)$ is a logit model. Given n training samples, $\{(x_i, y_i),\ i = 1, \ldots, n\}$, where $x_i \in \Re^m$ is an m-dimensional feature vector, and $y_i \in \{0, 1\}$ is a class label. Let π_i denote $p(y_i = 1|x_i, \beta)$, then an LR model is defined as follows:

$$\log \frac{\pi_i}{1 - \pi_i} = \beta_0 + \sum_{j=1}^{m} \beta_j x_{ij} \quad \Leftrightarrow \quad \pi_i = \frac{1}{1 + e^{-(\beta^T x)}} \tag{2}$$

where $\beta = (\beta_0, \beta_1, \ldots \beta_m)$ denotes the vector of regression coefficients including a constant β_0. The S-shape function of the LR model (see Eq. (1)) shown in Fig. 2 indicates a relative low probability of event occurrence (e.g., engine failure) until the threshold is reached, at which time the probability of the failure occurrence increases rapidly. In general, the S-shape curve describes well the health degradation tendency of a machine in its whole life. LR can be used well for prediction of the probability of an event occurrence by fitting data to a logistic curve, e.g., S-shape curve. Thus, LR is very appropriate for assessment and prediction of machine health.

The parameter estimation for β can be obtained by using the maximum likelihood method [39] based on the following negative log-likelihood probability (NLLP).

$$l(\beta) = \sum_{i=1}^{n} -y_i \beta^T x_i + \log\left(1 + \exp\left(\beta^T x_i\right)\right) \tag{3}$$

To avoid over-fitting and multicollinearity existing generally in the LR we often impose a penalty on large fluctuations of the estimated regression coefficients β. A penalization LR can be introduced in the objective function through using the most popular ridge penalty [40].

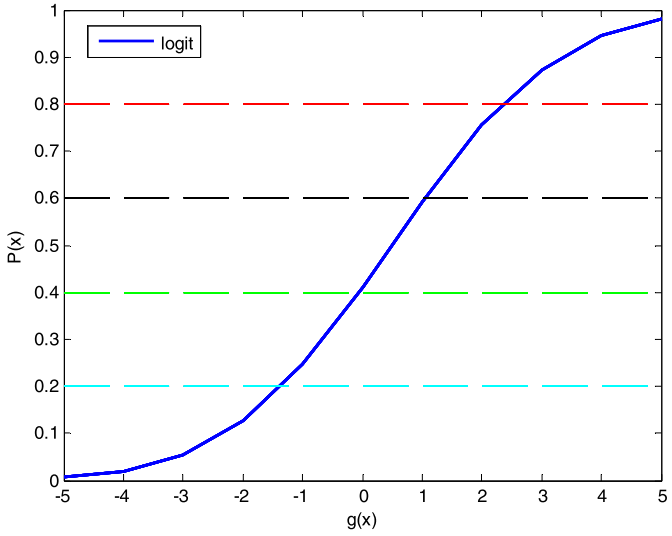

Fig. 2. Logistic function.

$$l^*(\beta) = l(\beta) + \frac{\lambda}{2}\|\beta\|^2 \tag{4}$$

where λ is the regularization parameter. In this study, λ is set up as a value 0.1 to obtain a good balance between the prediction performance and the penalization of the resulting LR.

Maximum likelihood estimation, $\hat{\beta}$, is obtained by maximizing l^* with respect to β. Through getting the derivatives of l^* with respect to β to zero and using Newton–Raphson algorithm to iteratively solve Eq. (4), an updating formulate is given as follows:

$$\begin{aligned} \beta^{new} &= \left(X^T W X + \lambda I\right)^{-1} X^T W R \\ R &= X\beta^{old} + W^{-1}(y - p) \end{aligned} \tag{5}$$

where $X \in \Re^m$ is an input data matrix (i.e., training dataset) with n vectors, W is the $n*n$ weight matrix with entries $p(\beta^{old}, x_i)(1 - p(\beta^{old}, x_i))$ on the diagonal and I is the identity matrix. Iterate to calculate p and R to obtain a new β until the change from β^{new} to β^{old} is less than the convergence criterion.

3.2. LRPR-based prognostic feature selection

Feature selection is a key step in the procedure of prognostics system modeling [41,42]. Mainly, the degrading propagation of aging component or system is reflected by the monitoring variables derived from sensor data. A very important part in engine health prognostics is to select a small subset of features which can effectively represent different health states of engines.

In this study, β in the LR gives the estimation of the regression coefficients and its absolute values indicate the relative importance of the input features. With the penalization learning of β in LRPR, the features with the smallest absolute values in β are eliminated. The candidate features and ages of engines are used as the inputs and outputs of the LR, respectively. The top ranked features will be selected and then used along with all the training set to design a predictor for the health prognostic purpose. The LRPR-based prognostic feature selection algorithm named LRPR-FS is presented as follows:

Algorithm I: LRPR-FS

Input: a training dataset $X = [x_1, ..., x_n]$ with m features $[f_1, ..., f_m]$ and the ages of engines $Y = [1, ..., T]$

Output: a feature subset.

(1) $X \leftarrow (X - \min(X))/(\max(X) - \min(X))$ // X is normalized
(2) $Y \leftarrow Y/T$ // Y is normalized and T is the life of the engine
(3) $[\beta_0, \beta_1 ..., \beta_m] \leftarrow LRPR(X, Y)$ // Run LRPR to obtain the parameters $\beta = [\beta_1, ..., \beta_m]$
(4) $\tilde{\beta} \leftarrow Sort(abs(\beta))$ // Sort the m features in a descending order of the absolute $[\beta_1, ..., \beta_m]$
(5) Select the top ranked r $(r \leq m)$ features based on $\tilde{\beta}$ and then output a feature subset.

3.3. Logistic probability-based health indicator

In statistics, LR is used for probability prediction of an event occurrence by fitting data to a logistic curve. Its prediction probability is constrained in a range from 0 to 1 and its probability curve presents S-shape (see Fig. 1), which is very suitable for describing engine health states. Thus, the LP, i.e., the output of LR (see Eq. (1)) is used as the health indicator to assess engine health states online. In order to improve the sensitivity and reliability of the LP to small health changes in engines, exponentially weighted moving average (EWMA) statistic [43] of the LPs is further employed as an improved health indicator,

$$ewma(t) = (1 - \alpha)ewma(t - 1) + \alpha * LP(x_t) \tag{6}$$

where $LP(x_t)$ is the output of LR (see Eq. (1)), and a smoothing constant $\alpha(0.2)$ is used to get a good balance between the historic information and the current observation.

3.4. Logistic regression-based long-term prediction

This section aims to predict engine health changes at the time t once the health indicator LP exceeds a predetermined threshold of slight degradation (i.e., δ_s), and further the engine RUL can be predicted with a predetermined threshold of engine failure (i.e., δ_f). Given the historical LPs $(LP_1, LP_2, ..., LP_t)$ and the corresponding engine ages $(1, 2, ..., t)$, the RUL predictor aims to estimate the future value $\hat{LP}_{t+h}$. Thus, LR is used to construct the relationship between the engine health states and ages. For multi-steps-ahead prediction, recursive approach is the most intuitive and simple way. Under this approach, it repeatedly performs one-step-ahead predictions until the desired horizon is reached. Eq. (7) expresses LR-based h-steps-ahead prediction:

$$\hat{LP}_{t+h} = LR(t + h) \tag{7}$$

The engine age (t) and health indicator (LP_t) are used as the input and output of the LR, respectively. With the constructed LR at the time t, the h-steps-ahead prediction can be performed by using Eq. (7). Once $\hat{LP}_{t+h}$ exceeds the threshold of engine failure (i.e., δ_f), the RUL prediction will be finished. LR need adapt to the health changes of engine and then to provide an accurate long-term prediction. When the time point moves ahead, LR will be re-constructed by using those historic data in a moving window with the size of 24 data points (the size of the moving window can be set up based on a balance between the prediction performance and the training time of LR), and then it is used to predict engine RUL. Each such learning procedure is called an epoch. It is desired that LR is constructed adaptively based on the newest trend of the health variable on time flow, which is particularly true in the case of long-term prediction. Such learning can adapt to the basic trend of engine health changes to perform an effective long-term prediction.

4. Particle filtering-based engine health prediction

4.1. State evolution modeling based on state-space-model

The recursive Bayesian estimation technique offers a general rigorous framework for dynamic system state-estimation. Its core

idea is to construct a probability density function (PDF) of the system states based upon all available process information [44,45]. Due to the flexibility of SSM for solving those complex prediction problems, there is an increasing interest in the modeling of SSM for long-term time series [4,23]. In this study, the propagation of the engine health can be modeled by the SSM with outputs being conditionally independently. The SSM can be written as follows:

$$x_k = f_k(x_{k-1}) + \omega_k \tag{8}$$

$$y_k = h_k(x_k) + \nu_k \tag{9}$$

where x_k represents the system state at time k, f_k is a state transition function, y_k is the system output (or measurement), h_k is a possibly nonlinear function that represents a mapping relationship between the system state and the noisy measurements, and ω_k and ν_k are the samples following independent noise distributions. Given the system measurement y_k, the objective of the state estimation in the SSM is to sequentially compute the state vector x_k.

In statistics, the aim of the state estimation in the SSM is to derive $p(x_k|y_{1:k-1})$ based on the probability function of the state x_k. Suppose that the state PDF $p(x_{k-1}|y_{1:k-1})$ is available at time $k-1$, $p(x_k|y_{1:k-1})$ can be achieved sequentially through continuous estimation and updating. The PDF of the prior state for the next time k by using the Chapman–Kolmogorov equation can be achieved for the estimation step:

$$p(x_k|y_{1:k-1}) = \int p(x_k|x_{k-1})p(x_{k-1}|y_{1:k-1})dx_{k-1} \tag{10}$$

where $p(x_k|x_{k-1})$ is defined via Eq. (8).

When a new measurement y_k is available, the marginal filtering density $p(x_k|y_{1:k})$ can be calculated by using the Bayes theorem as follows:

$$\begin{aligned} p(x_k|y_{1:k}) &= \frac{p(y_k|x_k)p(x_k|y_{1:k-1})}{p(y_k|y_{1:k-1})} \\ &\propto p(y_k|x_k)p(x_k|x_{k-m:k-1})p(x_{0:k-1}|y_{1:k-1}) \end{aligned} \tag{11}$$

where $p(y_k|y_{1:k-1})$ is the normalizing factor and can be calculated:

$$p(y_k|y_{1:k-1}) = \int p(y_k|x_k)p(x_k|y_{1:k-1})dx_k \tag{12}$$

where the likelihood function $p(y_k|x_k)$ is defined by Eq. (9).

Eqs. (10)–(12) constitute the formal solution to the problem of Bayesian recursive state-estimation. For a linear system with Gaussian noise, the above estimation can be performed by using the regular KF. For nonlinear/non-Gaussian systems, however, there are no closed-from solutions for the recursive state-estimation and thus those approximate methods (e.g., PF) have been employed recently [44]. PF is capable of identifying those nonlinear prediction model parameters in the state estimation procedure. Then, the identified system can be used for system state forecasting, e.g., engine RUL prediction.

4.2. Integration of logistic regression in particle filtering

PF is an effective technique for implementing the recursive Bayesian filtering via Monte Carlo simulation, in which a sequential importance sampling (SIS) algorithm is often used. As a powerful method for sequential time series analysis, PF approximates the PDF of the system state by using masses (i.e., particles) with associate weights based on the sequential sampling and Bayesian theory [45,46]. Based on a set of particles representing the estimation values from the unknown state space and a set of associated weights denoting discrete probability masses, the approximation of the posterior distribution $p(x_k|y_{1:k})$ is as follows [45,46]:

$$p(x_k|y_{1:k}) \approx \sum_{i=1}^{N} w_k^i \delta(x_k - x_k^i) \quad \text{with} \sum_{i=1}^{N} w_k^i = 1 \tag{13}$$

where x_k^i $(i = 1, 2, ..., N)$ is one of the N particles with the corresponding importance weight w_k^i (a higher weight indicates a higher sample probability), and $\delta(\bullet)$ is Dirac delta measure.

If the particles x_k^i $(i = 1, 2, ..., N)$ are drawn from the importance PDF $\pi(x_{0:k}, |y_{1:k})$, the particle weights are updated as follows:

$$w_k^i \propto \frac{p(x_k^i|y_{1:k})}{\pi(x_k^i|y_{1:k})} = w_{k-1}^i \frac{p(y_k|x_k^i)p(x_k^i|x_{k-1}^i)}{\pi(x_k^i|x_{k-1}^i, y_k)} \tag{14}$$

When the importance density is approximated as $p(x_k|x_{k-1})$, Eq. (14) becomes:

$$w_k^i \propto w_{k-1}^i p\left(y_k|x_k^i\right) \tag{15}$$

A Gaussian kernel function is often used for updating the weights:

$$w_k^i = w_{k-1}^i \frac{1}{\sqrt{2\pi}\sigma_v} \exp\left(-\frac{1}{2}\left[\frac{(y_k - h_k(x_k^i))}{\sigma_v}\right]^2\right) \tag{16}$$

where σ_v is the standard deviation of the measurement noise. In PF, after running some steps, the weights of some particles become trivial and then stop contributing to estimation of the overall system. Thus, residual resampling [47] is inserted in the estimation procedure so that the particles with negligible weights are replaced with those from the high-density area of the desired posterior distribution. Because the standard SIS algorithm is used in the proposed PF model, its convergency can be ensured effectively [48,49].

PF has been used for those prognostic applications in recent years [4,23], where it is employed to identify the linear or nonlinear system parameters during the state estimation period. However, some limitations associated with these classical PF-based predictors are that the prediction model parameters cannot be updated online in the prognostics procedure, or linear state functions are often used in the SSM [50]. As a result, the identified system model might not be robust, and then the prediction accuracy could be low in many applications, especially in long-term predictions with limited measurements. These obvious limitations associated with those PF-based machine health prognostics methods, however, can be properly reduced through employing the data-model-fusion scheme and online learning technique. Some papers discussed these advantages and disadvantages of the data-driven and model-based methods for machine health predictions [4,50,51].

The proposed prognostic framework aims to integrate the model-based (i.e., PF) and data-driven (i.e., LR) methods, which obtains strengths of each method while overcoming their respective disadvantages. To achieve such goal, the dynamic nonlinear predictor (i.e., LR) models the engine health changes online, and then is integrated in the PF framework. The engine health prediction is accomplished by the following integration of the LR in the PF:

$$x_k = \hat{x}_k + \omega_{k-1} \tag{17}$$

$$\hat{x}_k = LR_k(t_k) \tag{18}$$

where $LR_k(t_k)$ is a nonlinear function denoted by the LR predictor (see Section 3.4), t_k is the engine age, and the prediction output of the LR plus the process noise ω_{k-1} is the state of a Markov process at the next time. Thus, the PF integrates LR model in the SSM (i.e., Eq. (17) and (18)) to implement the long-term prediction for engine health. The Markov process noise ω is a stochastic

variable that can be assumed to follow a Gaussian distribution $\omega \sim N(\mu_\omega, \sigma_\omega)$. The prediction error could occur when the LR attempts to estimate the degradation growth of the engine (see Eq. (17)). Thus, the Markov process noise $\omega_k \sim N(\mu_\omega^k, \sigma_\omega^k)$ is a stochastic variable, and should be updated online to further improve the prediction accuracy of the LR predictor. The online updating of ω_k at time k is given based on exponentially weighted moving average method:

$$\mu_\omega^k = \alpha r_k + (1-\alpha)\mu_\omega^{k-1} \tag{19}$$

$$\sigma_\omega^k = \alpha\sqrt{\frac{\sum_{i=0}^{n-1}(r_{k-i} - \mu_\omega^{k-i})^2}{n}} + (1-\alpha)\sigma_\omega^{k-1} \tag{20}$$

where r_k is the residual between the actual degradation quantification value and the prediction value of the LR at time k, n is the number of the prediction residuals, and α ($\alpha = 0.1$ is used in this study) is a smoothing parameter to give a big weight to the current observation. The Markov process noise $\omega_k \sim N(\mu_\omega^k, \sigma_\omega^k)$ will be updated in the RUL prediction procedure based on the engine health changes online. According to the balance of the smoothing of the degradation tendency and the convergence performance of the proposed model, the initial μ_ω and σ_ω are assigned the value 0.001 and 0.005, respectively. Therefore, the PF model will be updated online due to the using of the data-model-fusion scheme and the adaptive updating of the Markov process noise ω_k.

4.3. Application procedure of the proposed system

The application procedure of the proposed engine health prognostics system is presented as follows:

Step 1: Collect the healthy and degraded data from the historic engines.

Step 2: LRPR-FS is implemented to select the prognostic features from all available sensor variables as the inputs of the baseline LR.

Step 3: Construct the baseline LR to implement engine health assessment.

Step 4: The output (i.e., LP) of the baseline LR is calculated for the current observation to assess the engine health state.

Step 5: If the LP indicates that the engine health is in degraded state, the RUL prediction will be triggered.

Step 6: The SSM that models the health propagation of engines is constructed based on the LR and state estimation technique.

Step 7: The degradation growth model (see Eq. (18)), represented by the LR and the process noise, is used by the PF to generate a set of particles. The key parameters of PF are set up as follows: The 500 particles are generated; The initial μ_ω and σ_ω of the process noise ω_{k-1} are assigned the value 0.001 and 0.005, respectively; The residual resampling [47] is used; The particle rejection method is not used.

Step 8: Based on the values of the particles and their corresponding weights, one-step-ahead prediction is implemented as follows:

$$\tilde{x}_k = \sum_{i=1}^{N} w_{k-1}^i x_k^i \tag{21}$$

The h-steps-ahead prediction can be implemented at each cycle k by successively taking the expectation of the model update Eq. (21) for future time points in the following:

$$\tilde{x}_{k+h} = E(x_{k+h}^i) = \sum_{i=1}^{N} w_{k+h}^i x_{k+h}^i \tag{22}$$

$$x_{k+h}^i = LR(t_{k+h-1}) + \omega_{k+h-1} \tag{23}$$

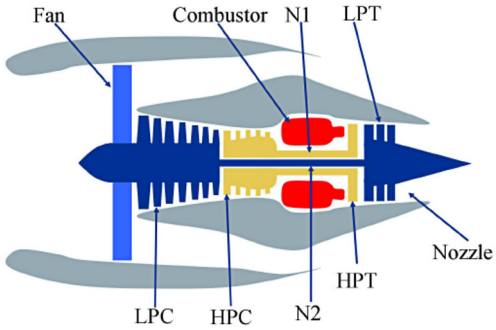

Fig. 3. Diagram of engine in C-MAPSS.

where $\tilde{x}_{k+h}$ is the h-steps-ahead prediction value, E is the expectation of x_{k+h}^i, x_{k+h}^i is the state value of the ith particle at the time t_{k+h}, w_{k+h-1}^i is the weight of the ith particle at the $k+h-1$th time instant, and N is the number of particles. $LR()$ is the constructed LR model online, and it's age (i.e., t_{k+h-1}) and LP (i.e., x_{k+h-1}^i) input can be recursively obtained by using Eq. (18). When a new health indicator value (i.e., LP) becomes available, the weights of all particles are updated by using Eq. (16). Then, resampling is performed.

Step 9: With the current prediction residuals, update the process noise ω_k using Eq. (19) and (20).

Step 10: Based on the particle set at time k, $\{x_k^i\}_{i=1}^N$ and the pre-defined failure threshold ($\delta_f = 0.95$ is used in this study), the cumulative failure distribution function ($F(k)$) [4] can be approximated by the following:

$$F(k) \approx \frac{number\ of\ x_k^i : x_k^i \geq \delta_f\ (i = 1, 2, ..., N)}{N} \tag{24}$$

Step 11: Repeat Steps 6–10 until the RUL prediction $\tilde{x}_{k+h}$ meets the failure threshold at an engine cycle, and the engine health prognostics will be completed. Finally the predicted RUL (see Eq. (22)) and the predictive RUL distribution $P(x_{k+h}|y_{1:k})$ (see Eq. (25)) can be achieved at the time point $k+h$.

$$P(x_{k+h}|y_{1:k}) \approx \sum_{i=1}^{N} w_k^i \delta(x_{k+h} - x_{k+h}^i) \tag{25}$$

5. Experiment and result analysis

To identify and quantify the current health state of a deteriorating engine is a key factor to ensuring high efficient operation. A case study based on a turbofan engine health degradation simulation dataset is implemented to verify the effectiveness of the proposed prognostics system.

This case study was conducted on a turbine engine degradation simulation model C-MAPSS developed at NASA [52], a representative simulation model of a modern commercial turbofan engine (see Fig. 3). C-MAPSS has 14 inputs and 13 health parameters that let users to simulate the effects of different health deteriorations in any of five rotating components in the engine, i.e., fan, LPC, HPC, HPT and LPT. The system outputs consist of various sensor response surfaces and operability margins. Each data record (i.e., a 24-element vector) includes 3 values for the system operability settings and 21 values for engine health measurements, which are all contaminated by noise. Although there are total 21 sensor variables that are available in the dataset, we select sixteen variables that are currently available onboard for many commercial turbofan engines for health prognostics in this study (see Table 1). Six different flight conditions were set up in this experiment, comprising a range of values for the following three operational settings:

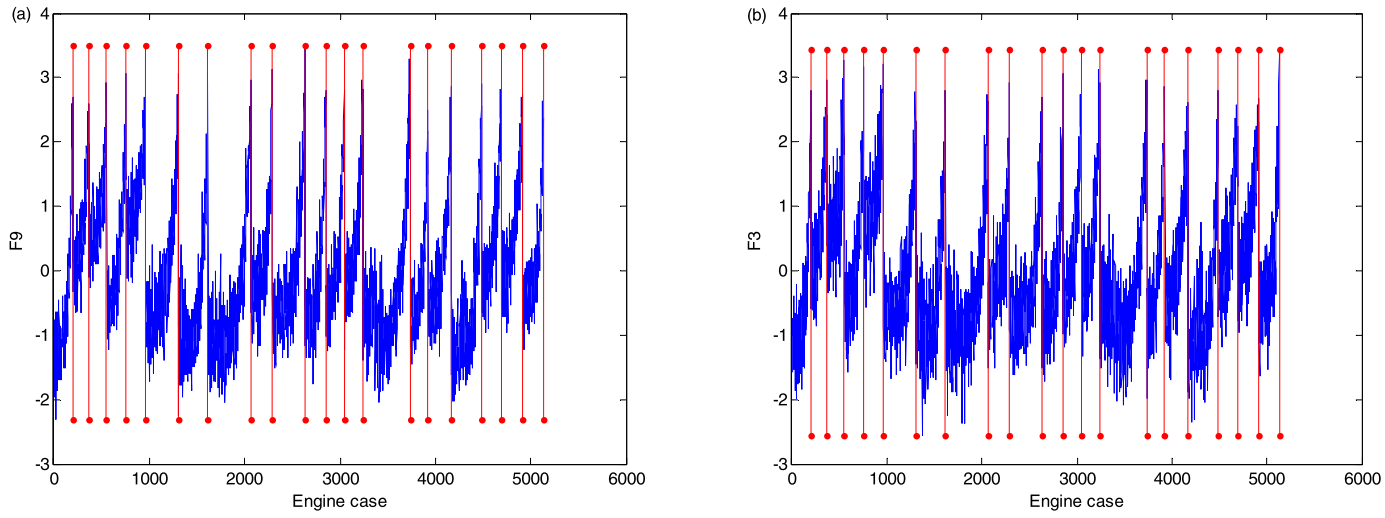

Fig. 4. Sensor variable in the full life of each engine: (a) F9 (Ps30), and (b) F3 (T50).

Table 1
Sixteen selected variables in C-MAPSS to measure system response.

No.	Variable	Description	Units
F1	T24	Total temperature at LPC outlet	°R
F2	T30	Total temperature at HPC outlet	°R
F3	T50	Total temperature at LPT outlet	°R
F4	P15	Total pressure in bypass-duct	psia
F5	P30	Total pressure in HPC outlet	psia
F6	Nf	Physical fen speed	rpm
F7	Nc	Physical core speed	rpm
F8	Epr	Engine pressure ratio (P50/P2)	–
F9	Ps30	Static pressure at HPC outlet	Psia
F10	phi	Ratio of fuel flow to Ps30	Pps/psia
F11	NRf	Corrected fen speed	rpm
F12	NRc	Corrected core speed	rpm
F13	BPR	Bypass ratio	–
F14	htBleed	Bleed enthalpy	–
F15	Nf_dmd	Demanded fan speed	rpm
F16	W32	LPT coolant bleed	lbm/s

altitude (Alt: 0–42K ft), Mach number (M: 0–0.84), and throttle resolver angle (TRA: 20–100). Each engine is running normally at the start of each time series, and then develops a different initial defect at different time points because of different degrees of various initial wears and manufacturing variation in practice. The magnitude of the fault grows gradually until the engine system failures finally. We verify effectiveness of the proposed prognostics system on the 70 representative engines (the 20 engines of them are used to construct a baseline LR and the other 50 engines named Engine #1–#50 are used to perform health prognostics, respectively) with a compressor subjected to gradual health deteriorations in service.

5.1. Engine health degradation assessment

The LRPR-FS will be firstly performed to select the prognostic features by using the sensor data of all twenty historic engines. For each engine, the sensor data and the corresponding ages in its full life are used as the inputs and outputs of LRPR-FS, respectively. The ranked features are obtained by using LRPR-FS. From this result, the first two important prognostic features are F9 (i.e., Ps30) and F3 (i.e., T50), respectively. Fig. 4 presents F9 and F3 variable in the full life of each engine. The vertical axes of Fig. 4 (a) and (b) are the sensor variable values, i.e., Ps30 and T50, respectively. The horizontal axes of Fig. 4 are the used 20 engine cases for training the baseline LR, where the red lines separate the sensor data of each engine (i.e., the segment of the two red lines is the full life internal of each engine). It is obvious from Fig. 4 that the two features have very good trendability in the full life of the engines, which are two important indications for evaluating effectiveness of the prognostic features [53]. In contrast, the features F15 (Nf_dmd) and F16 (W32) ranked in the last two features can not present good trendability in the full life of the engines (see Fig. 5) because they present different increasing or decreasing tendency for different engines. This verifies that LRPR-FS is capable of selecting the effective prognostic features.

The top 10 ranked features by LRPR-FS are used as the inputs of LR. The full life cycle data are input to the baseline LR to implement engine health monitoring. The LPs are generated by the baseline LR (see Eq. (1)) for the full life of each engine (i.e., the four representative engines Engine #1–#4) and then are plotted in Fig. 6. The degradation propagation of each engine is presented clearly in Fig. 6. The slight degradation line 0.4 and the failure line 0.95 are also plotted in Fig. 6, which should be set up based upon the requirements of real applications. It can be observed clearly from Fig. 6 that: (1) The whole health propagation of engines in their full life is achieved obviously from health, slight degradation, to failure in which the failure probability (i.e., LP) increases consistently as engine health deteriorates continuously over time series flow; (2) LP is capable of recognizing the early degradation occurring in each engine when it exceeds the slight degradation threshold, which allows users to have enough maintenance time to take some effective measurements to respond prior to those catastrophic failures in the engines; (3) In addition, although the life and failure modes are different in each engine, the LP still consistently describes the whole health degradation behavior from 0 to 1 in their full life. Therefore, the health indicator (i.e., LP) provides an effective monitoring in the full life of engines based upon the comprehensible quantifying values and its good tendency.

For the purpose of comparison, we implement a testing using all the features as inputs of the LR to further analyze the effectiveness of LRPR-FS-based feature selection for improving the performance of the LP. Fig. 7 presents the LP charts for the four representative engines #1–#4, where all features are used as the inputs of the baseline LR. It can be observed from Fig. 7 that the LPs are approaching 0.5 and 0.9 when the engine is in healthy state and failure state, respectively. In contrast, the LPs in Fig. 6 are approaching 0.3 and 0.95 when the engine is in healthy state and failure state, respectively. The comparison between Fig. 6 and Fig. 7 indicates that the LP with selected features shows better health assessment results than that of the LP with all features. This comparison further indicates that the prognostic feature selection

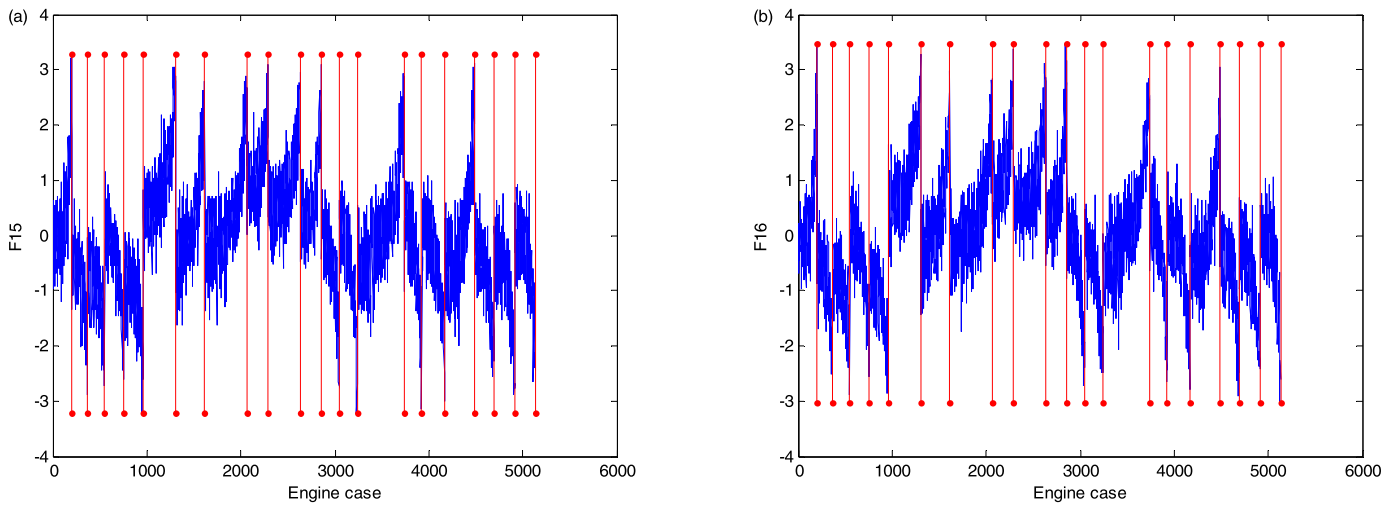

Fig. 5. Sensor variable in the full life of each engine: (a) F15 (Nf_dmd), and (b) F16 (W32).

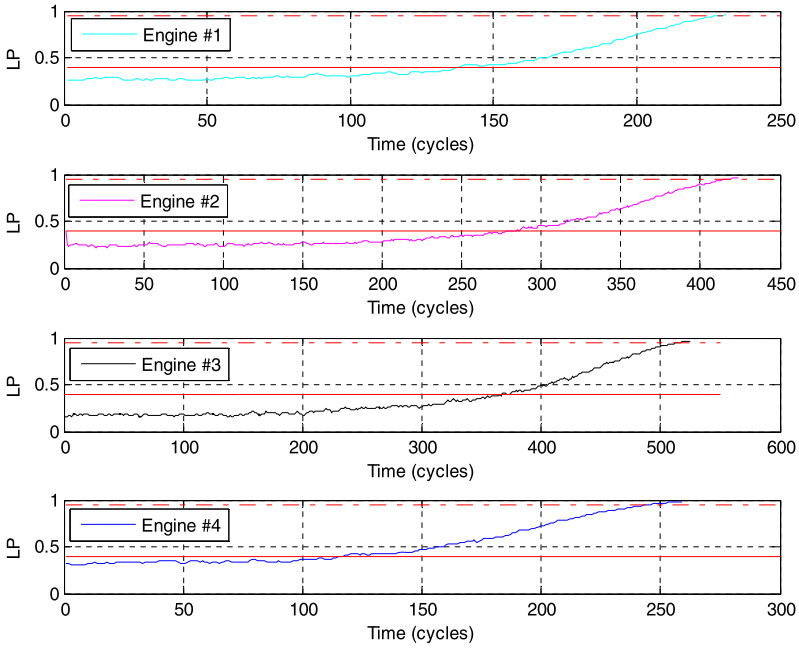

Fig. 6. Health indicator curve output by LP indication for Engine #1–#4.

based on LRPR-FS is a key step in improving the performance of the prognostics system.

Although these sensor variables show monotonic trend (see Fig. 4), it is hard to use one of them directly as the HI indicator because they can not provide the above characteristics of the LP indicator (see Fig. 6). Thus, a fusion of these sensor variables is important to improve the effectiveness of the HI. Furthermore, we provide the comparison between the LR and the back-propagation network (BPN) for engine health assessment to further approve the effectiveness of the LR in the proposed system. BPN is a typical stochastic model and has been used for machine health assessment [54]. Thus, it is appropriate to compare the proposed method with the BPN for engine health assessment. The BPN structure consists of an input layer with 10 nodes for the 10 input features, one hidden layer with 15 hidden nodes, and an output layer with 1 node for the health indicator. The number of iterations is 500. The hyper tangent (tansig) and sigmoid (logsig) functions were used as the activation functions of the hidden and output layer, respectively. The same training dataset of the LR is also used to train the BPN. Fig. 8 and 9 present the health indicator values (not the EWMA statistics) of the LR and BPN for the two representative engines #1 and #3, respectively. It is clear that the LR outperforms the BPN for engine health assessment. The LP shows smaller variations in the healthy phase of the two engines than that of the BPN. More important is that the LP indication provides a better tendency of the health degradation assessment for the full life of these engines in comparison with that of the BPN.

Meanwhile, we implemented another comparison between LP and minimum quantization error (MQE) based on SOM using unsupervised learning scheme [55]. MQE is the Euclidean Distance of the input and the best matched map of the SOM trained by the healthy data. The following parameters are set up for SOM training. The number of the map units is 300. The distance function is the Euclidean distance weight function. The topology function is the Hextop function. The ordering phase steps of the SOM are 500. The healthy data (i.e., the first 50 samples of the used 20 engines) are used to construct SOM. Fig. 10 presents the MQE values for the two representative engines #1 and #3. It is clear from Fig. 8,

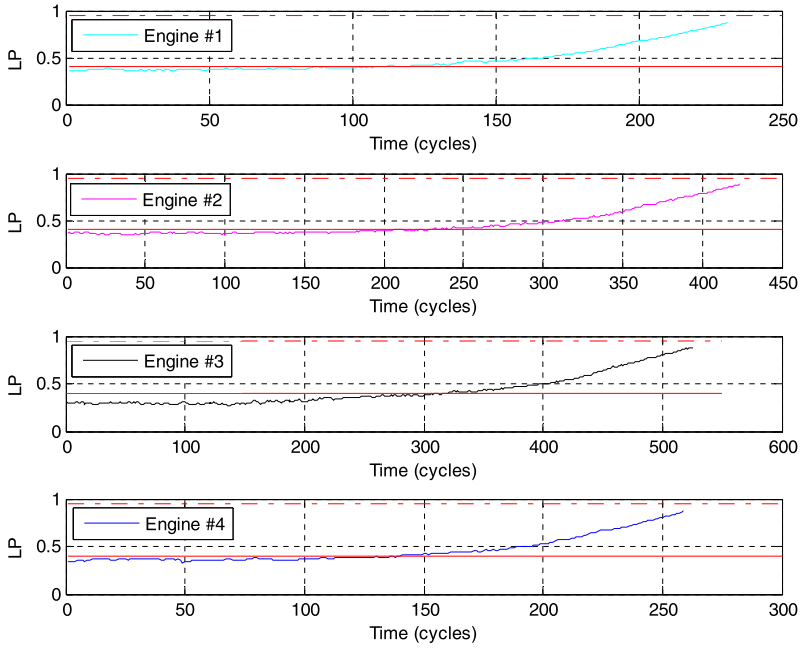

Fig. 7. Health indicator curve output by LP indication with all features for Engine #1–#4.

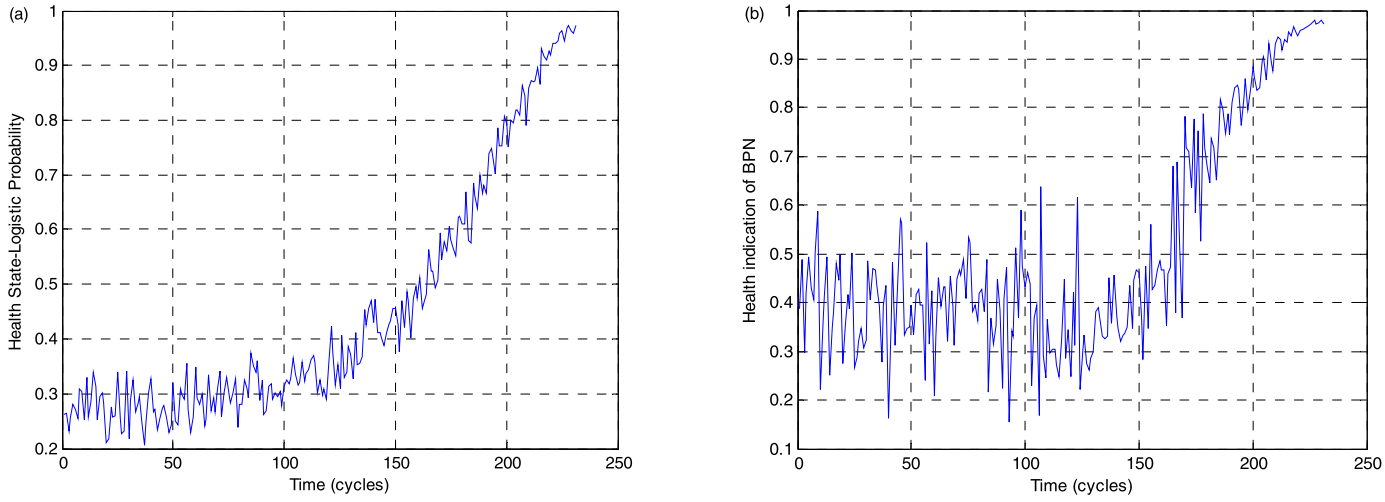

Fig. 8. Health indicator curve of the LR and the BPN for Engine #1, (a) LR, and (b) BPN.

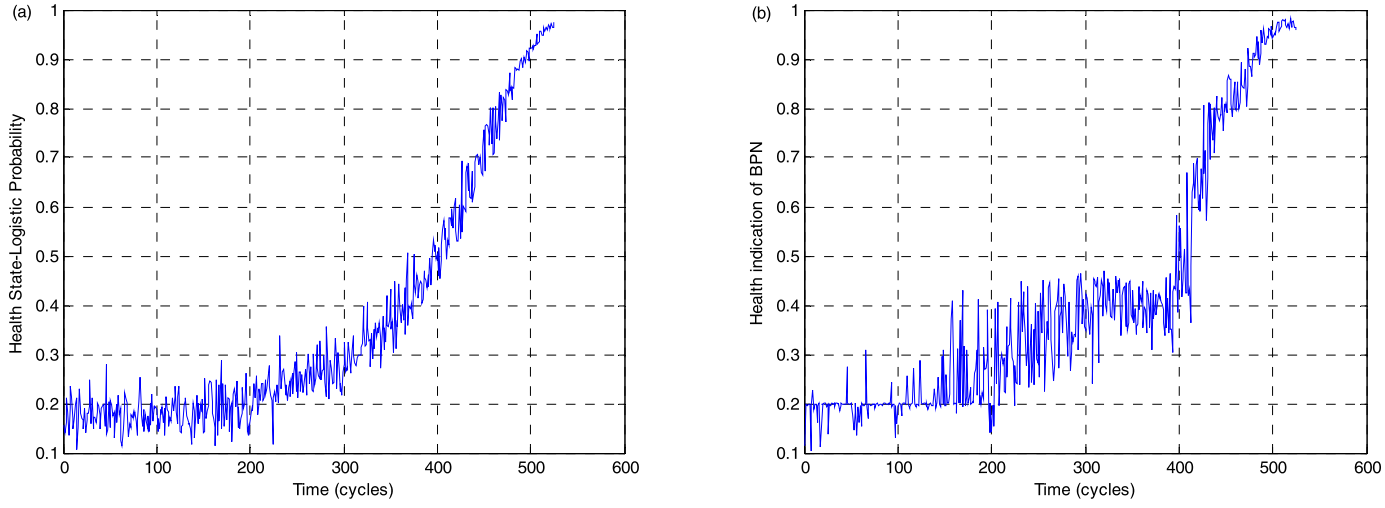

Fig. 9. Health indicator curve of the LR and the BPN for Engine #3, (a) LR, and (b) BPN.

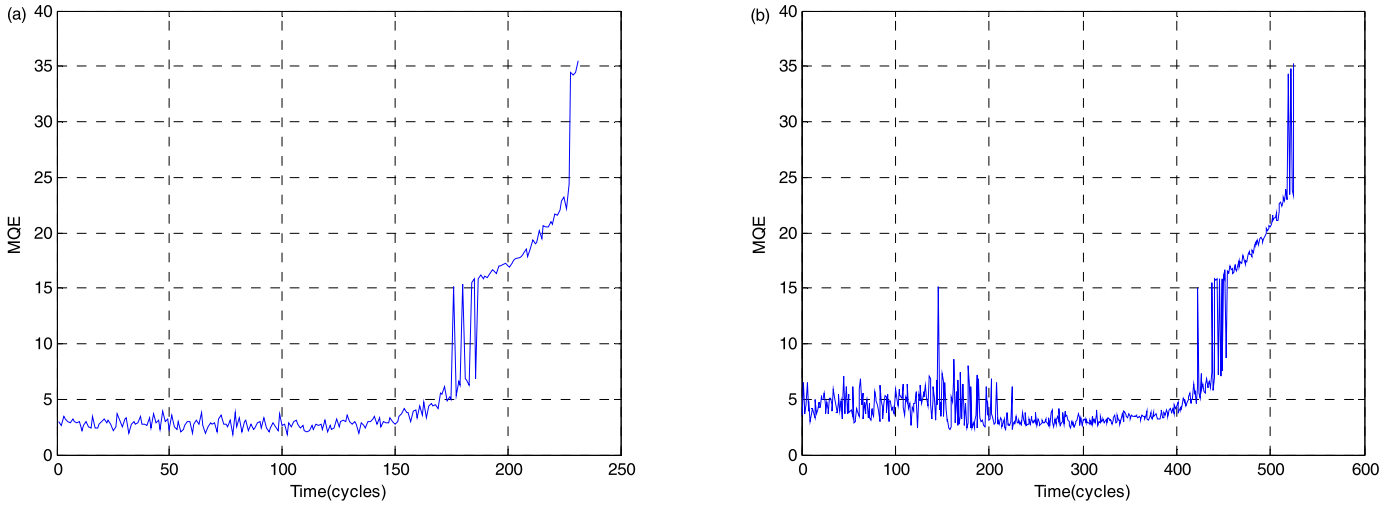

Fig. 10. Health indicator curve of MQE for Engine #1 and #3, (a) Engine #1, and (b) Engine #3.

9 and 10 that LP chart shows better performance than MQE chart for engine health.

5.2. Long-term prediction

The performance of the proposed prognostics method for long-term prediction is firstly tested on Engine #1 and #3. The 5-steps-ahead and 10-steps-ahead predictions are performed when the window moves ahead with 5 and 10 time-steps after the slight degradation alarms are triggered, respectively. For the purpose of comparison, LR, BPN, GPR and RVM [56] are considered to perform the long-term prediction. A GPR model is an example of the use of a flexible, probabilistic, non-parametric model for the uncertainty prediction of output-variable distributions [57].

RVM is a Bayesian form representing a generalized linear model of identical functional form of SVM. RVM and GPR have been used recently in the machine health prognostics [25,36]. The modeling scheme of the proposed method is also used for LR, BPN, RVM and GPR. A Gaussian kernel function with the length scale (10) is used in RVM [56]. The number of iterations for RVM is 300. A Gaussian covariance function is used in GPR [57]. The number of iterations for GPR is 300. The BPN structure consists of an input layer with 1 node, one hidden layer with 5 hidden nodes, and an output layer with 1 node. The number of iterations is 500. The hyper tangent (tansig) and sigmoid (logsig) functions were used as the activation functions of the hidden and output layer, respectively.

Fig. 11 shows the 5-steps-ahead prediction results and the corresponding absolute prediction errors of the proposed method, LR, BPN, RVM and GPR for Engine #1. It can be observed that the proposed method captures the dynamics of the engine's health changes quickly and accurately, the predicted values are close to the actual values, and the prediction becomes more accurate when it is close to the final failure time point. The absolute errors of the proposed method, LR, BPN, RVM and GPR are 0.0116, 0.0159, 0.0451, 0.0562 and 0.0201, respectively. Apparently, the proposed method outperforms the LR, BPN and RVM from Fig. 11. Moreover, the proposed method provides more important health information, e.g., RUL uncertainty analysis. Thus, the proposed method is more effective for long-term prediction than LR, BPN, RVM and GPR. Fig. 12 presents the 10-steps-ahead prediction results of the proposed method, LR, BPN, RVM and GPR for Engine #3, respectively. The absolute errors of the proposed method, LR, BPN, RVM and GPR are 0.0119, 0.0124, 0.0504, 0.1273 and 0.0433, respectively. The proposed method can effectively capture and track the health degradation propagation and thus outperforms the LR, BPN, RVM and GPR. This result further illustrates that the proposed method is very effective to perform long-term prediction.

5.3. RUL and RUL probability distribution prediction

To further illustrate the RUL prediction ability of the proposed system, the final failure time points of Engine #1–#10 are predicted by the proposed system at different life cycles. In this study, the RUL prediction will be performed once the slight degradation alarm is triggered. This is derived by projecting out failure probability estimation of each particle from the current time t into the future until they hit the predetermined failure threshold of 0.95. Finally, the engine RUL can be obtained as the predicted failure time minus the current time.

To verify the prediction performance of the proposed prognostics system, Engine #2 subjected to gradual health deterioration in service is considered. Suppose that one RUL prediction is performed at cycle 295 of Engine #2 (10% of the remaining life after the slight degradation alarm is triggered). The health assessment and prediction results are presented in Fig. 13(a). Due to the statistical nature of the Bayesian method used in this study, the prediction results are all in distribution forms approximated by 500 particles. The mean of the health prediction is represented by the dashed line in Fig. 13(a). Moreover, the 95% confidence bound (i.e., the pre-defined failure threshold $\delta_f = 0.95$) for the prediction is also given in this figure. It should be noted that the setup of the failure threshold should be based on the real requirements in the applications. It can be observed from Fig. 13(a) that the proposed prognostics system detects a certain trend or change in the underlying parameters, and then traces the degradation propagation based on those new arrival measurements. Thus, the prediction starting at cycle 295 that is the early life phrase can still produce good results. This can be attributed to the flexible SSM technique, which assumes neither a regular pattern nor the stability of the underlying degradation propagation, but does include the dynamic system propagation, such as the nonlinear changes in the health deterioration of Engine #2. The predicted failure time is 540, and thus the predicted RUL of Engine #2 is 245 cycles ($540 - 295 = 245$). The accuracy of the prediction is 72.64% according to the following testing standard:

$$Accuracy = \left(1 - \frac{|t_a - t_p|}{t_a}\right) \times 100\% \tag{26}$$

where t_a and t_p are the actual life and predicted life of the engine, respectively. The other three RUL predictions of Engine #2 at cycle

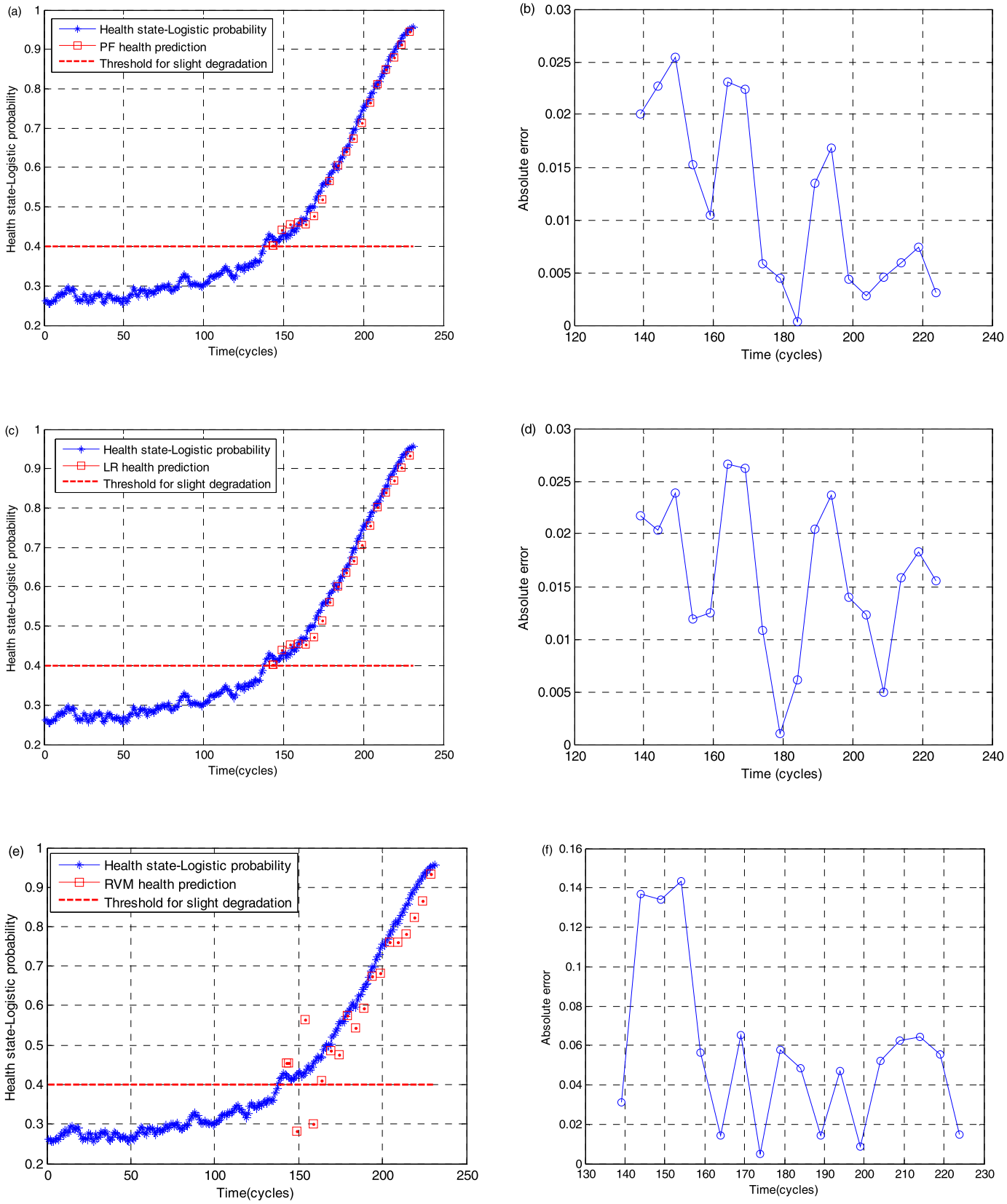

Fig. 11. The 5-steps-ahead prediction of the proposed method, LR and RVM on Engine #1, (a) the proposed method prediction, (b) error of the proposed method prediction, (c) LR prediction, (d) error of the LR prediction, (e) RVM prediction, (f) error of the RVM prediction, (g) BPN prediction, (h) error of the BPN prediction, (i) GPR prediction, and (j) error of the GPR prediction.

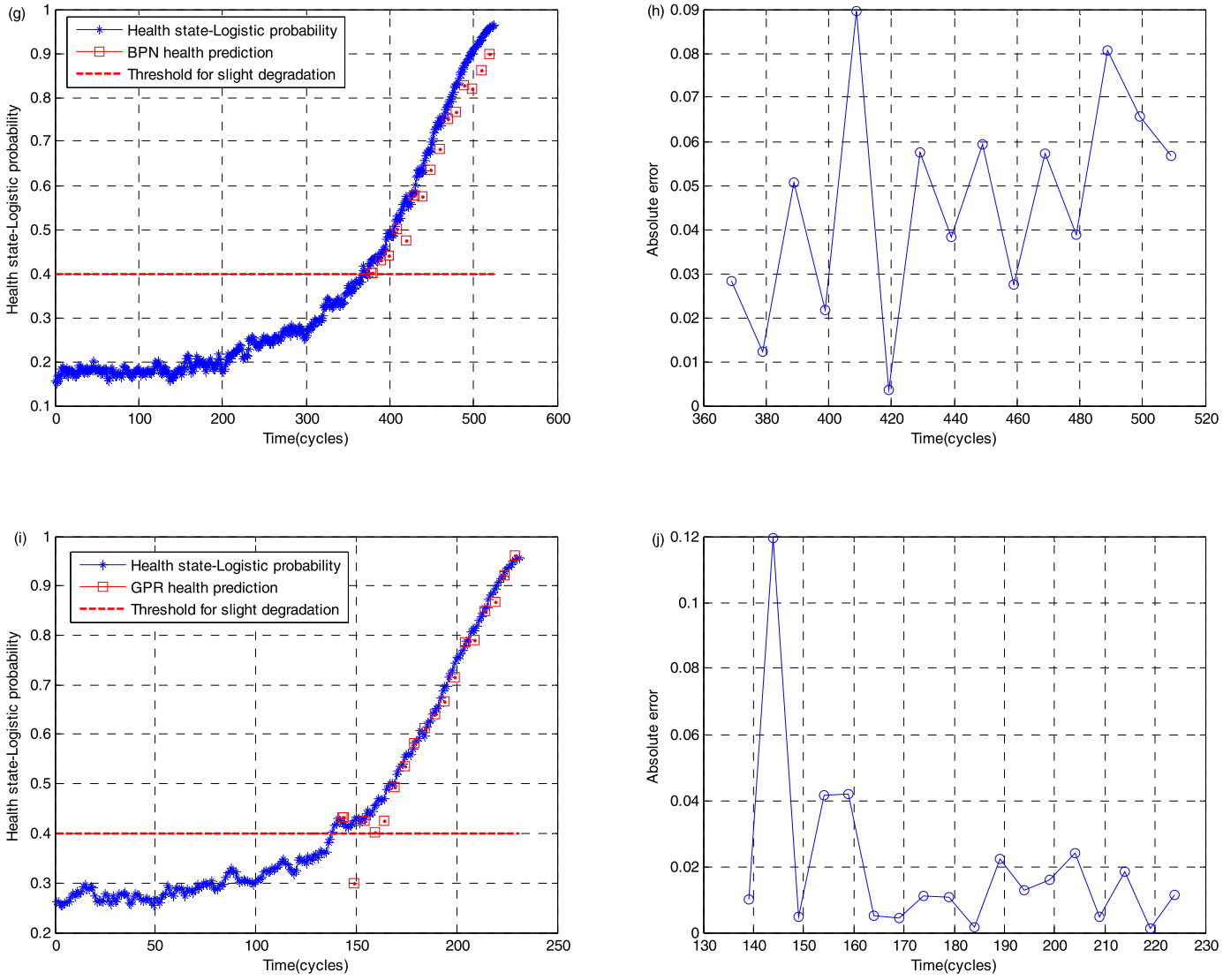

Fig. 11. (*continued*)

323 (30% of the remaining life), cycle 352 (50% of the remaining life) and cycle 381 (70% of the remaining life) are also performed to further illustrate the effectiveness of the proposed method. As new measurements are obtained and the trend of the health indicator becomes steeper (see Fig. 13(b)–(d)), the proposed method detects the change and then adjusts the prediction accordingly because of the using of the data-model-fusion scheme. The predicted failure time at cycle 323, 352 and 381 is 514, 470 and 432, respectively. Thus, the three RUL predictions are 191 ($514 - 323 = 191$), 118 ($470 - 352 = 118$), and 51 ($432 - 381 = 51$), respectively. The accuracy of the three predictions is 79.01%, 89.15% and 98.11%, respectively. The prediction becomes more accurate when it is close to the final failure time point, as the predicted failure cycle matches with the real value, and the standard deviation of the RUL prediction is reduced to 8 cycles, meaning that the confidence level of the prediction increases. Even if the accuracy is optimistic and acceptable in industrial applications, the predicted RUL is longer than the actual RUL. This is a common problem encountered in implementing multi-steps-ahead prediction. However, the multi-steps-ahead prediction is of necessity for those real applications of machine health prognostics.

The RUL PDF is further computed by fitting a mixture of Gaussians to the RUL values generated by the particle population, which is approximated by a histogram-based the probability distribution, i.e., the number of particles whose values locate in the range 0 and 1 divides by 500. Fig. 13 further shows the RUL PDF prediction of the proposed method at the predicted failure time point of each engine. It can be seen from this figure that the proposed method gives good prediction of the failure time with small uncertainty, and the more accurate predictions are obtained when the moving window is approaching the end time point of the engine. It is meaningful for users to provide the RUL PDF prediction because it offers more engine health information, i.e., RUL uncertainty.

Fig. 14 presents more details with regard to the RUL prediction made at cycle 323 and 381 for Engine #2. The predictive health degradation paths are given in Fig. 14(a) and (c), and are represented by many particle evolution paths. According to the predictive distribution of the health state, the cumulative time-to-failure distribution from Eq. (25) is presented in Fig. 14(b) and (d). If necessary, techniques like kernel density estimation can be employed to smooth the distribution to get the PDF of the failure time.

To further illustrate the RUL prediction ability of the proposed method, the failure time prediction for Engine #1–#10 at different phrases (i.e., 10%, 30%, 50% and 70%) of the remaining life is implemented after triggering the slight degradation alarms. To test the

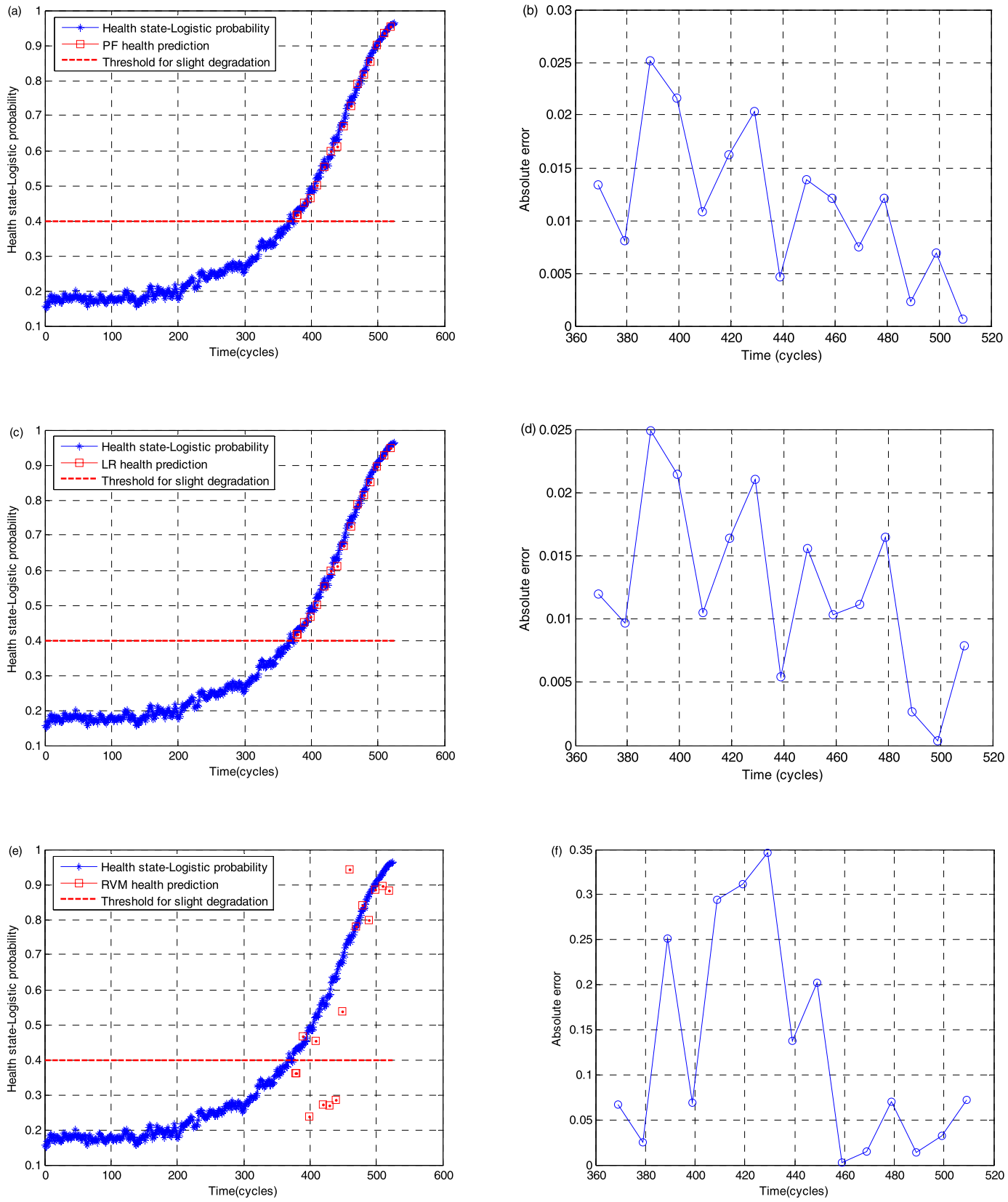

Fig. 12. The 10-steps-ahead prediction of the proposed method, LR and RVM on Engine #3, (a) the proposed method prediction, (b) error of the proposed method prediction, (c) LR prediction, (d) error of the LR prediction, (e) RVM prediction, (f) error of the RVM prediction, (g) BPN prediction, (h) error of the BPN prediction, (i) GPR prediction, and (j) error of the GPR prediction.

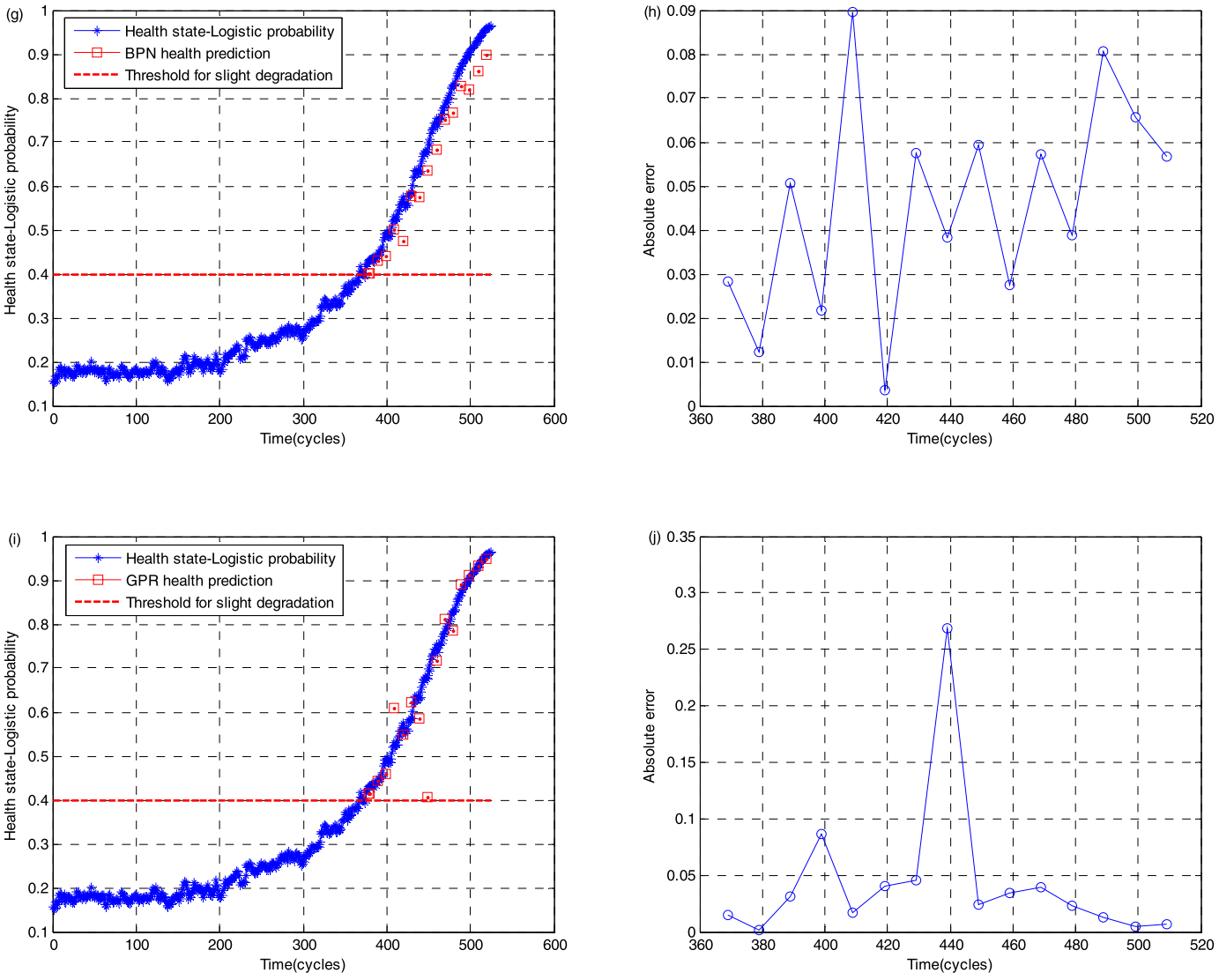

Fig. 12. (*continued*)

Table 2
The failure time prediction, prediction accuracy and steadiness index for Engine #1–#10 at different phrases (10%, 30%, 50% and 70%) of the remaining life after triggering the slight degradation alarm (AL is the actual life of engines).

No.	Prediction time (% of the remaining life)					Prediction accuracy (%) at 70% of the remaining life	Steadiness index
	10%	30%	50%	70%	AL		
Engine #1	330	413	282	252	231	90.91	3.1
Engine #2	540	513	470	432	424	98.11	3.9
Engine #3	671	591	547	547	525	95.81	4.1
Engine #4	494	338	287	288	259	88.80	4.7
Engine #5	514	522	451	425	409	96.09	4.1
Engine #6	673	554	376	358	321	88.47	3.5
Engine #7	350	351	279	273	246	89.02	2.4
Engine #8	385	433	328	287	253	86.56	4.9
Engine #9	620	533	514	507	481	94.59	4.6
Engine #10	431	530	346	304	275	89.45	4.9

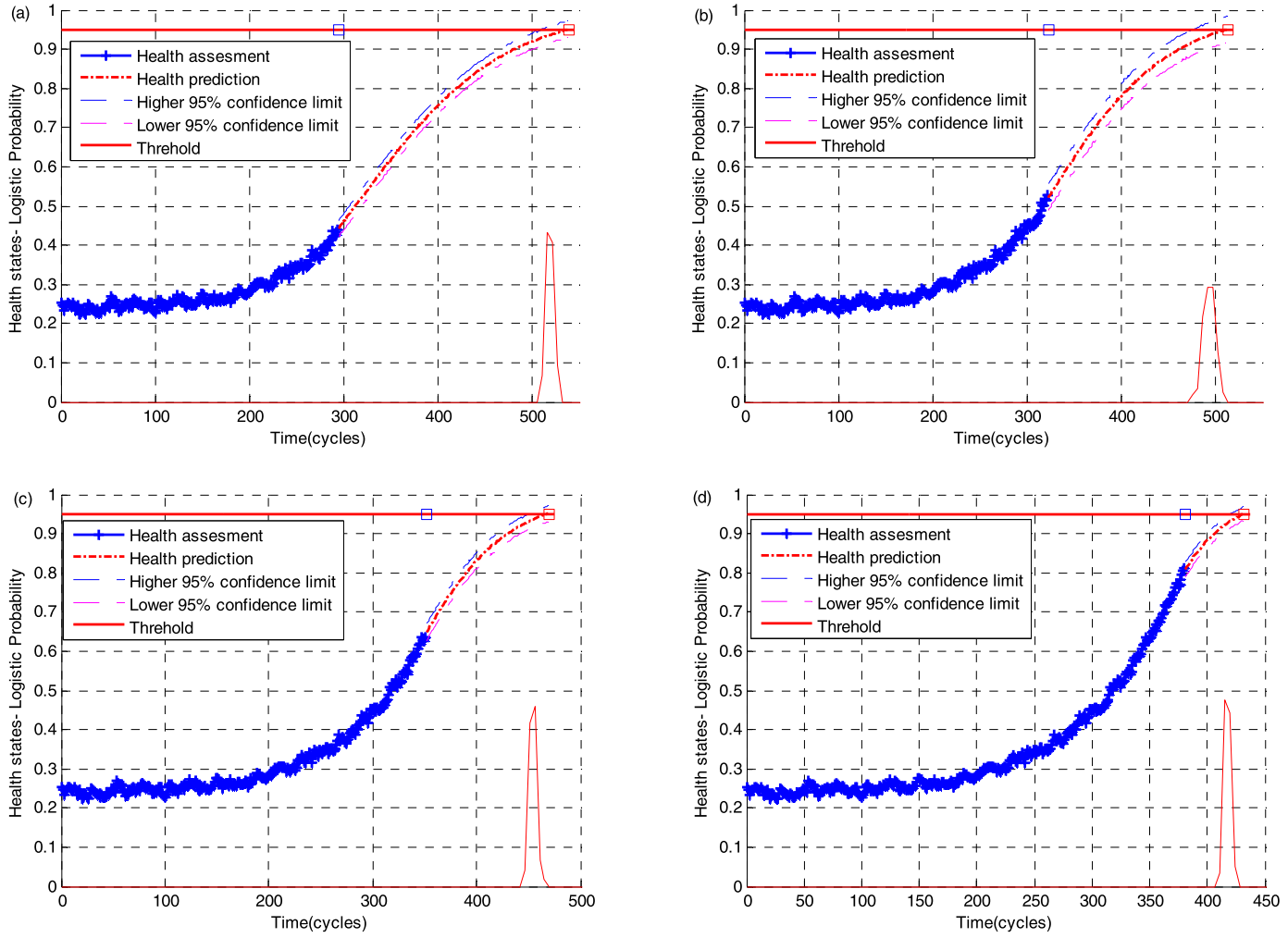

Fig. 13. RUL prediction for Engine #2 at (a) Cycle 295 (10% of the remaining lifetime), (b) Cycle 323 (30% of the remaining lifetime), (c) Cycle 352 (50% of the remaining lifetime), and (d) Cycle 381 (70% of the remaining lifetime).

steadiness of the proposed method, the steadiness index (SI) [27] is also calculated as follows:

$$SI = \sqrt{\text{var}(RUL_{(t-\Delta t):t})} \tag{27}$$

where RUL is the predicted engine RUL, t is the prediction time point, Δt is the sliding time moving and $\Delta t = 5$ is used to test the steadiness of the proposed method. Small values of SI indicate more stable RUL prediction is. The prediction results of the proposed method are presented in Table 2. The prediction accuracy and SI at the 70% phrases of the full life show that the prediction is good and the RUL prediction variation is small. As the moving window moves ahead, the prediction accuracy has consistently improved as shown in Table 2. When approaching the end of engine life, the predictions become closer to the actual failure time and the prediction uncertainty decreases simultaneously (see Fig. 12). This is because the LP chart gives more stable assessment results in the last life phrase of each engine, and the learning of the prognostics model is more effective and then it can make more accurate prediction for shorter-term future.

Finally, we implement a comparison between the proposed method and the PF with BPN (or RVM) (i.e., the LR predictor is replaced with the BPN or RVM predictor in the proposed model) on the RUL prediction of Engine #1–#50 at different phrases (i.e., 30% and 70%) of the remaining life. Table 3 presents the mean prediction accuracy of these methods. These methods can be compared smoothly because the similar experimental setup is used by them for this case. We can see from Table 3 that the proposed method shows the best prediction performance among the other three methods. This further indicates that the design scheme of the proposed method is successful for improving the engine RUL prediction performance.

Table 3
The mean prediction accuracy (%) on Engine #1–#50 at different phrases (30% and 70%) of the remaining life after triggering the slight degradation alarm.

Method	Prediction time (% of the remaining life)	
	30%	70%
The proposed method	52.34	90.10
PF with BPN	47.67	85.67
PF with RVM	41.45	80.45

6. Conclusions

This paper proposes a novel engine health prognostics system based on a probabilistic health indicator and SSM with an integration of LR and PF. A baseline LR is applied to model the complex distribution space of the collected sensor variables selected by LRPR. A probabilistic interpretation (i.e., LP) of the current en-

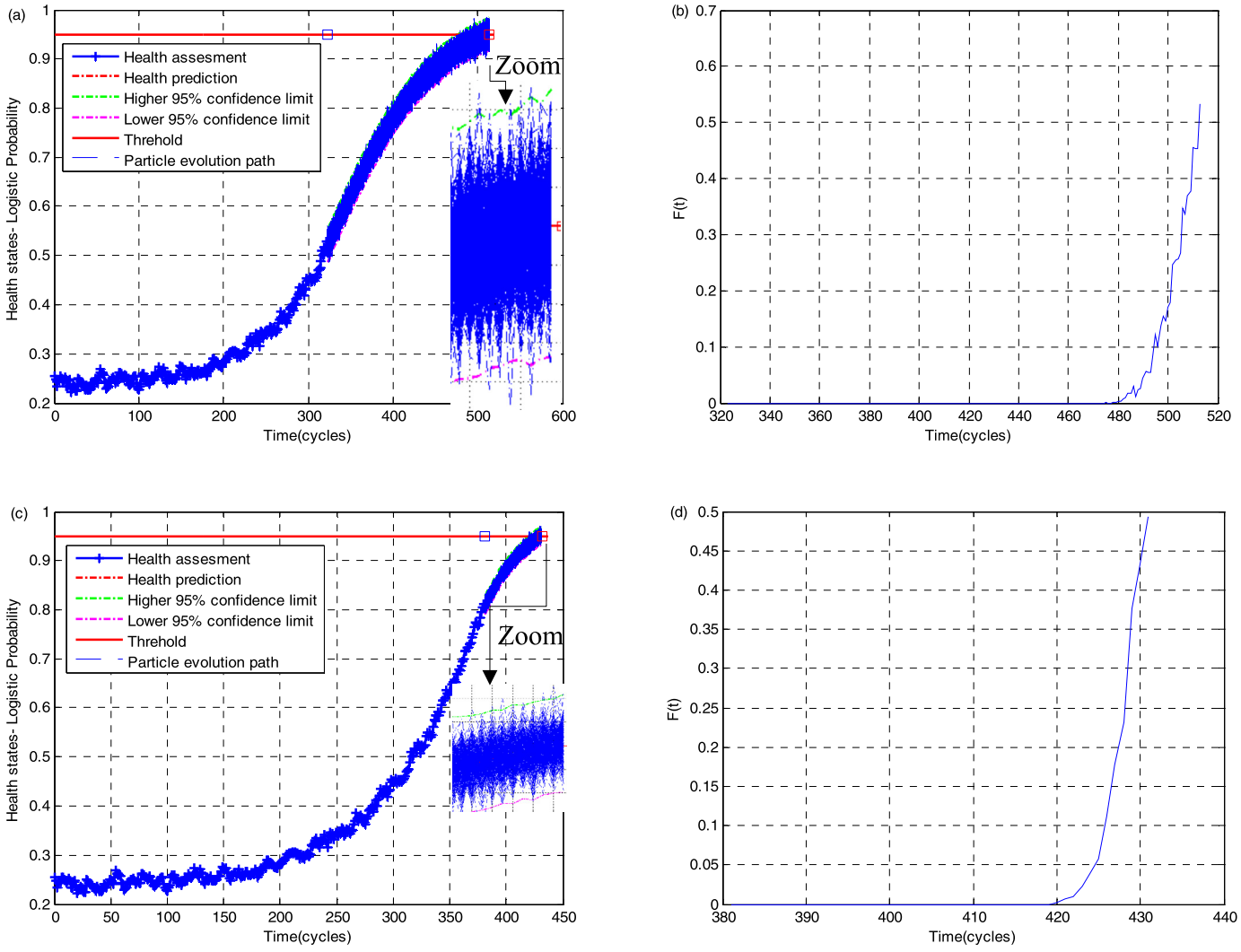

Fig. 14. RUL distribution prediction for Engine #2, (a) Health prediction at Cycle 323 (30% of the remaining lifetime), (b) Cumulative failure function at Cycle 323 (30% of the remaining lifetime), (c) Health prediction at Cycle 381 (70% of the remaining lifetime), (d) Cumulative failure function at Cycle 381 (70% of the remaining lifetime).

gine health state is realized, which would provide comprehensible health information to operators. The experimental results verify that a consistent and pragmatic degradation indicator with good comprehensibility can be effectively extracted by the LP indication derived from the baseline LR, even at an engine defect's early stage. An SSM based on a data-model-fusion is applied to online dynamic model of engine health degradations. A PF that combines the LR predictor and the process noise is developed to represent the health degradation process. These design schemes reduce some obvious limitations associated with those PF-based machine health prognostics methods. Therefore, the major contribution of this paper is the proposed data-model-fusion-based engine health prognostics method including prognostic feature selection, model updating online, probability-based health indicator and data-model-fusion, enable it to adaptively learn the health degradation model to various engine running dynamics quickly and then to implement an effective health assessment and RUL prediction. The experimental results based on the gas turbines on C-MAPSS test-bed indicate that the proposed system is effective for engine health prognostics. However, these are some potential limitations existing in the proposed method, e.g. LR reconstruction online, supervised learning-based LR for generating health indicator, which could be eliminated in the future studying.

Conflict of interest statement

The authors declared that they have no conflicts of interest to this work.

Acknowledgement

This research was supported by the National Natural Science Foundation of China (No. 51375290), Shanghai Aerospace Science and Technology Innovation Foundation (No. SAST2015054), and the Fundamental Research Funds for the Central Universities.

References

[1] J. Yu, Local and nonlocal preserving projection for bearing defect classification and performance assessment, IEEE Trans. Ind. Electron. 59 (5) (2012) 2363–2376.

[2] M.J. Roemer, C.S. Byington, G.J. Kacprzynski, G. Vachtsevanos, An Overview of Selected Prognostic Technologies with Application to Engine Health Management, ASME GT2006-90677, 2006.

[3] D. Dimogianopoulos, J. Hios, S. Fassois, Aircraft engine health management via stochastic modelling of flight data interrelations, Aerosp. Sci. Technol. 16 (1) (2012) 70–81.

[4] J. Sun, H. Zuo, W. Wang, M.G. Pecht, Application of a state space modeling technique to system prognostics based on a health index for condition-based maintenance, Mech. Syst. Signal Process. 28 (4) (2012) 585–596.

[5] E. Mohammadi, M. Montazeri-Gh, A fuzzy-based gas turbine fault detection and identification system for full and part-load performance deterioration, Aerosp. Sci. Technol. 46 (2015) 82–93.
[6] X. Fang, R. Zhou, N. Gebraeel, An adaptive functional regression-based prognostic model for applications with missing data, Reliab. Eng. Syst. Saf. 133 (0) (2015) 266–274.
[7] R. Kurz, K. Brun, Degradation of gas turbine performance in natural gas service, J. Nat. Gas Sci. Eng. 1 (3) (2009) 95–102.
[8] P.G. Nieto, E. Garca-Gonzalo, F.S. Lasheras, F. de Cos Juez, Hybrid PSOSVM-based method for forecasting of the remaining useful life for aircraft engines and evaluation of its reliability, Reliab. Eng. Syst. Saf. 138 (0) (2015) 219–231.
[9] Y.G. Li, P. Nilkitsaranont, Gas turbine performance prognostics for condition-based maintenance, Appl. Energy 86 (10) (2009) 2152–2161.
[10] X. Wang, U. Kruger, G.W. Irwin, G. McCullough, N. McDowell, Nonlinear PCA with the local approach for diesel engine fault detection and diagnosis, IEEE Trans. Control Syst. Technol. 16 (1) (2008) 122–129.
[11] J.E. Yoon, J.J. Lee, T.S. Kim, J.L. Sohn, Analysis of performance deterioration of a micro gas turbine and the use of neural network for predicting deteriorated component characteristics, J. Mech. Sci. Technol. 22 (12) (2008) 2516–2525.
[12] S. Gupta, A. Ray, S. Sarkar, M. Yasar, Fault detection and isolation in aircraft gas turbine engines. Part 1: underlying concept, Proc. Inst. Mech. Eng., G J. Aerosp. Eng. 22 (3) (2008) 307–318.
[13] D. Simon, D.L. Simon, Constrained Kalman filtering via density function truncation for turbofan engine health estimation, Int. J. Syst. Sci. 41 (2) (2010) 159–171.
[14] C.J. Li, H. Lee, Gear fatigue crack prognosis using embedded model, gear dynamic model and fracture mechanics, Mech. Syst. Signal Process. 19 (4) (2005) 836–846.
[15] G.F. Harrison, M.E.F. Smith, J. Hurse, Procedure of aero engine component life usage prediction, in: AIDAA/AAAF/DGLR/RAeS 5th European Propulsion Forum, Pisa, Italy, 1995.
[16] G.F. Harrison, Translation of service usage into component life consumption, in: Recommended Practices for Monitoring Gas Turbine Engine Life Consumption, RTO Technical Report 28 (RTO-TR-28, AC/323/(AVT)TP/22), 2000.
[17] R. Moghaddass, M.J. Zuo, An integrated framework for online diagnostic and prognostic health monitoring using a multistate deterioration process, Reliab. Eng. Syst. Saf. 124 (2014) 92–104.
[18] D. Simom, A comparison of filtering approaches for aircraft engine health estimation, Aerosp. Sci. Technol. 12 (4) (2008) 276–284.
[19] D. Simon, D.L. Simon, Aircraft turbofan engine health estimation using constrained Kalman filtering, J. Eng. Gas Turbines Power 127 (2) (2005) 323–328.
[20] D.L. Simon, S. Garg, Optimal turner selection for Kalman filtering based aircraft engine performance estimation, J. Eng. Gas Turbines Power 132 (3) (2010) 031601.
[21] F. Lu, H. Ju, J. Huang, An improved extended Kalman filter with inequality constraints for gas turbine engine health monitoring, Aerosp. Sci. Technol. 58 (2016) 36–47.
[22] B. Pourbabaee, N. Meskin, K. Khorasani, Sensor fault detection, isolation, and identification using multiple-model-based hybrid Kalman filter for gas turbine engines, IEEE Trans. Control Syst. Technol. 24 (4) (2016) 1184–1200.
[23] B. Saha, K. Goebel, S. Poll, J. Christophersen, Prognostics methods for battery health monitoring using a bayesian framework, IEEE Trans. Instrum. Meas. 58 (2) (2009) 291–296.
[24] F. Cadini, E. Zio, D. Avram, Model-based Monte Carlo state estimation for condition-based component replacement, Reliab. Eng. Syst. Saf. 94 (3) (2009) 752–758.
[25] F. Li, J. Xu, A new prognostics method for state of health estimation of lithium-ion batteries based on a mixture of Gaussian process models and particle filter, Microelectron. Reliab. 55 (7) (2015) 1035–1045.
[26] H. Dong, X. Jin, Y. Lou, C. Wang, Lithium-ion battery state of health monitoring and remaining useful life prediction based on support vector regression-particle filter, J. Power Sources 271 (2014) 114–123.
[27] Y. Hu, P. Baraldi, F. Di Maio, E. Zio, A particle filtering and kernel smoothing-based approach for new design component prognostics, Reliab. Eng. Syst. Saf. 134 (2015) 19–31.
[28] Z. Xi, R. Jing, P. Wang, C. Hu, A copula-based sampling method for data-driven prognostics, Reliab. Eng. Syst. Saf. 132 (0) (2014) 72–82.
[29] K.L. Son, M. Fouladirad, A. Barros, E. Levrat, B. Iung, Remaining useful life estimation based on stochastic deterioration models: a comparative study, Reliab. Eng. Syst. Saf. 112 (0) (2013) 165–175.
[30] S. Sarkar, X. Jin, A. Ray, Data-driven fault detection in aircraft engines with noisy sensor measurements, J. Eng. Gas Turbines Power 133 (2011) 081602.
[31] R. Eustace, A real-world application of fuzzy logic and influence coefficients for gas turbine performance diagnostics, J. Eng. Gas Turbines Power 130 (6) (2008) 061601.
[32] E. Lapira, D. Brisset, D. Ardakani, D. Siegel, J. Lee, Wind turbine performance assessment using multi-regime modeling approach, Renew. Energy 45 (2012) 86–95.
[33] C. Zhang, N. Wang, Aero-engine condition monitoring based on support vector machine, Phys. Proc. 24 (2012) 1546–1552.
[34] G.J. Kacprzynski, M. Gumina, M.J. Roemer, D.E. Caguiat, T.R. Galie, A Prognostic Modeling Approach for Predicting Recurring Maintenance for Shipboard Propulsion Systems, ASME GT2007-27275, Jun. 2001.
[35] Y.G. Li, P.A. Nilkitsaranout, Gas Path Diagnostic and Prognostic Approach for Gas Turbine Applications, ASME, GT2007-27275, May 2007, pp. 573–584.
[36] F.D. Maio, K.L. Tsui, E. Zio, Combining relevance vector machine and exponential regression for bearing residual life estimation, Mech. Syst. Signal Process. 31 (8) (2012) 405–427.
[37] F. Li, J. Xu, A new prognostics method for state of health estimation of lithium-ion batteries based on a mixture of Gaussian process models and particle filter, Microelectron. Reliab. 55 (2015) 1035–1045.
[38] M. Alamaniotis, A. Grelle, L.H. Tsoukalas, Regression to fuzziness method for estimation of remaining useful life in power plant components, Mech. Syst. Signal Process. 48 (1) (2014) 188–198.
[39] W.M. Houston, D.J. Woodruff, Empirical Bayes Estimates of Parameters from the Logistic Regression Model, ACT Research Report Series 97-6, June 1997.
[40] A.E. Hoerl, R.W. Kennard, Ridge regression: application to nonorthogonal problems, Technometrics 17 (1) (1970) 69–82.
[41] J.H. Zhou, C.K. Pang, Z.W. Zhong, F.L. Lewis, Tool wear monitoring using acoustic emissions by dominant-feature identification, IEEE Trans. Instrum. Meas. 60 (2) (2011) 547–559.
[42] J. Yu, Health condition monitoring of machines based on hidden Markov model and contribution analysis, IEEE Trans. Instrum. Meas. 61 (8) (2012) 2200–2211.
[43] J.M. Lucas, M.S. Saccucci, Exponentially weighted moving average control schemes: properties and enhancements, Technometrics 32 (1) (1990) 1–12.
[44] D. Simon, Optimal State Estimation: Kalman, H, and Nonlinear Approach, Wiley–Interscience, 2006.
[45] M.S. Arulampalam, S. Maskell, N. Gordon, T. Clapp, A tutorial on particle filters for online nonlinear/non-Gaussian Bayesian tracking, IEEE Trans. Signal Process. 50 (2) (2002) 174–188.
[46] A. Doucet, S. Godsill, C. Andrieu, On sequential Monte Carlo sampling methods for Bayesian filtering, Stat. Comput. 10 (3) (2000) 197–208.
[47] J. Liu, R. Chen, Sequential Monte Carlo methods for dynamic systems, J. Am. Stat. Assoc. 93 (443) (1998) 1032–1044.
[48] A. Doucet, N.D. Freitas, Sequential Monte Carlo Methods in Practice, Springer, Berlin, 2001, pp. 15–88.
[49] D. Crisan, A. Doucet, A survey of convergence results on particle filtering methods for practitioners, IEEE Trans. Signal Process. 50 (3) (2002) 736–746.
[50] J. Liu, W. Wang, F. Ma, Y.B. Yang, C.S. Yang, A data-model-fusion prognostic framework for dynamic system state forecasting, Eng. Appl. Artif. Intell. 25 (4) (2012) 814–823.
[51] E. Walker, S. Rayman, R.E. White, Comparison of a particle filter and other state estimation methods for prognostics of lithium-ion batteries, J. Power Sources 287 (2) (2015) 1–12.
[52] A. Saxena, K. Goebel, Turbo fan engine degradation simulation dataset, retrieved from NASA Ames Prognostics Data Repository, http://ti.arc.nasa.gov/tech/dash/pcoe/prognostic-data-repository, NASA Ames, Moffett Field, CA, 2012.
[53] K. Javed, R. Gouriveau, N. Zerhouni, P. Nectoux, A feature extraction procedure based on trigonometric functions and cumulative descriptors to enhance prognostics modeling, in: Annual Conference of the Prognostics and Health Management, USA, 24–27 June 2009, pp. 1–7.
[54] J. Yan, C.X. Guo Wang, A dynamic multi-scale Markov model based methodology for remaining life prediction, Mech. Syst. Signal Process. 25 (4) (2011) 1364–1376.
[55] R. Huang, L. Xi, X. Li, C.R. Liu, H. Qiu, J. Lee, Residual life predictions for ball bearings based on self-organizing map and back propagation neural network methods, Mech. Syst. Signal Process. 21 (1) (2007) 193–207.
[56] M.E. Tipping, The relevance vector machine, in: Advances in Neural Information Processing Systems, vol. 12, MIT Press, Cambridge, MA, 2000, pp. 652–658.
[57] C.E. Rasmussen, C.K.I. Williams, Gaussian Processes for Machine Learning, MIT Press, Cambridge, MA, 2006.